Paper No. 118

ISMS2016

Numerical simulation for propagation characteristics of outburst shock wave and gas flow when outburst prevention facilities fail

Zhou Aitao[a,*], Wang Kai[b], Kong Yuyu[c], Liu Ang[d]

[a] School of Resource & Safety Engineering, State Key Laboratory of Coal Resources and Mine Safety, China University of Mining & Technology, Beijing,China 100083
[b] School of Resource & Safety Engineering, State Key Laboratory of Coal Resources and Mine Safety, China University of Mining & Technology, Beijing,China 100083
[c] Jincheng Zetai Safety Evaluation Center, Jincheng, Shanxi, China 048000
[d] School of Resource & Safety Engineering, State Key Laboratory of Coal Resources and Mine Safety, China University of Mining & Technology, Beijing,China 100083

ABSTRACT
In order to numerically simulate the propagation characteristics of outburst shock waves and gas flow when outburst prevention facilities fail, the propagation characteristics model of outburst shock waves and gas flow was established, and the mechanism of gas counter current was analyzed. The propagation characteristics of shock wave and gas flow at two types of geometry models were numerically simulated by using Fluent software. The results show that most of the gas flow produced by outbursts propagates to intake airways when crossheading with an excavation roadway at the same level; however, when crossheading with an excavation roadway not at the same level, gas is mainly discharged from the return airway, and the effect of the gas flow on the intake airway is small. The results have important theoretical and practical significance for mine disaster rescue and preventing secondary accidents.
KEYWORDS: outburst prevention facilities; shock wave and gas flow; gas counter current

1. INTRODUCTION

Shock waves and gas flow are formed during coal and gas outburst, which can induce casualties and property loss. Scholars have performed extensive study in this field. Cheng Wuyi (2004) made a simple theoretical analysis and mathematical deduction based on the forming process and propagation law of outburst shock wave and gas flow. For the dynamic process of the flow, F. Otuonye (1998) proposed a simplified mechanism of outburst and established the corresponding physical model. Wang Kai et al., 2011, Wang Kai et al., 2012, Zhou A.T(2012) systematically studied the formation mechanism and propagation characteristics of the shock wave and flow caused by outburst; based on theoretical analysis, experimental studies, and numerical simulations, they systematically analyzed the attenuation characteristics of the shock wave and gas flow from the outburst in a straight roadway, turning roadway, bifurcation roadway, and variable cross-section roadway. It is well known that when outburst prevention facilities fail, intake airway associate with the excavation airway where outburst occurs and then the shock wave and gas flow pour out from the crossheading into the intake airway (Zhang J, 2007). This paper mainly studies the impact of outburst shock waves and gas flow on the intake airway and proposes appropriate solutions. Firstly, the roadway model after the outburst prevention facilities was established and process of the shock wave and gas flow was numerically simulated. Secondly, the variation process with time of pressure, velocity, and density in observation points was monitored, and the conditions of pressure, velocity, density, and concentration variation of gas within roadways at different time were obtained. Thirdly, the impact of outburst shock wave and gas flow on the ventilation system after the air door failure was analyzed. The result obtained has important theoretical and practical significance for mine disaster rescue and the prevention of secondary accidents.

2. ANALYSIS OF PROPAGATION CHARACTERISTICS OF OUTBURST SHOCK WAVE AND GAS FLOW

The propagation of outburst shock wave and gas flow can be considered a one-dimensional compressible gas semitropical unsteady continuous flow, which is always accompanied by the movement of disturbance waves. When the disturbance waves propagate through media, physical quantities of shock wave and gas flow at any point change dramatically over time, forming unsteady movements. Therefore, in order to study the unsteady compressible flow of the shock wave and gas flow, one must study the disturbance wave motion.

*Corresponding author – email: cumtbzat@126.com

When gas outburst occurs, the intensity of the shock wave is changed. In other words, the velocity of the outburst shock wave is unchanging, and the gas parameters of the wave-after change over time. To convert the unsteady state to a steady state, it is necessary to coordinate the observation with the shock wave motion, and set up three basic equations for the control-body that surrounds the shock wave. Because the shock wave is extremely thin, its volume can be ignored. The rate of mass, kinetic energy, momentum and internal energy variation over time of the control-body and other items are equal to zero, and the variable intensity on both sides of the shock wave can also be analyzed using the equation of steady flow. This is equivalent to dividing the varying intensity movement process of a shock wave into some limited short moments. Now every small part can be dealt with as a stationary flow process, and this steady flow is known as quasi-steady flow.

Figure 1 is a transient state of a shock wave in the propagation process. The region where shock waves through is called the wave-after, and the region where there is no wave disturbance is known as the wave-front. The rightward direction represents the positive direction of flows. Velocity, pressure, density, enthral, and temperature of the wave-front and wave-after were v_1, p_1, ρ_1, h_1, T_1 and v_2, p_2, ρ_2, h_2, T_2, respectively, and the velocity of shock wave is v. The dotted area is the control plane area for the study of shock wave motion.

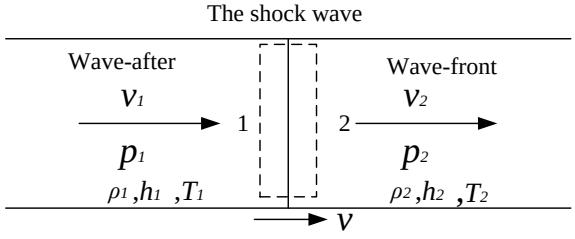

Figure 1: Shock wave communication status model.

Through coordinate conversion, the movement process of the shock wave is transited from unsteady flow into steady flow, namely, the coordinate system that flows with the shock wave is selected for reference, and the velocity of the shock wave becomes zero. At this time a standing vertical impulse wave is formed; the wave-after velocity becomes $v_1 - v$, direction to the left; the wave-front velocity also becomes $v_2 - v$, direction to the left; parameters of wave-after and wave-front are constant, as shown in Figure 2.

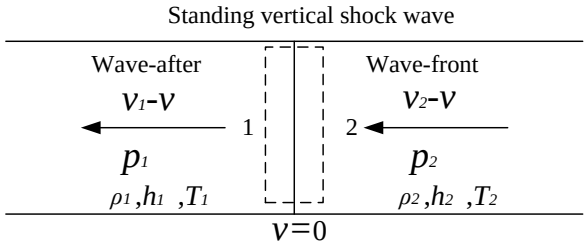

Figure 2: State model of standing vertical shock wave.

According to the state model of a standing vertical shock wave, firstly establish the continuity equation. According to the conservation of mass the continuous equation of a standing vertical shock wave is as follows:

$$\rho_1(v_1 - v) = \rho_2(v_2 - v) \tag{1}$$

Establish the momentum equation. The shock wave within the roadway belongs to the one-dimensional flow, and both sides of it are in the role of air and gas pressures, respectively. Ignoring the body force, the momentum equation of one-dimensional steady flow can be written as:

$$p_1 + \rho_1(v_1 - v)^2 = p_2 + \rho_2(v_2 - v)^2 \tag{2}$$

Establish the energy equation. Because airflow through the shock wave can be considered an adiabatic process, the total temperature T of the wave-front and wave-after can be considered as constant. Friction is negligible, and therefore the shock wave is very thin. For one-dimensional unsteady flow without shaft work and potential role, and $h = u + p/\rho$, the energy equation is as follows:

$$u_1 + \frac{p_1}{\rho_1} + \frac{(v_1 - v)^2}{2} = u_2 + \frac{p_2}{\rho_2} + \frac{(v_2 - v)^2}{2} \tag{3}$$

The three previous equations have seven unknowns：p_1, ρ_1, v_1, p_1, ρ_2, v_2 and v (Specific internal energy, u, can be obtained using the state equation $\mathrm{u} = \frac{1}{\gamma - 1} RT = \frac{1}{\gamma - 1}\frac{p}{\rho}$ derived by the the p and ρ). Four parameters are independent. Given any of these four parameters the rest can be uniquely identified. For example, p_2, ρ_2, v_2, and anyone parameter of wave-after is given, then the rest of the parameters and shock wave velocity can be uniquely identified. When putting these parameters into three equations the wave equation is obtained:

$$\left.\begin{aligned}
&\frac{\rho_1\rho_2}{\rho_1-\rho_2}(p_1-p_2)=-\rho_1^2(v-v_1)^2=-\rho_2^2(v-v_2)^2\\
&\frac{p_1}{p_2}=\frac{(\gamma+1)\rho_1-(\gamma-1)\rho_2}{(\gamma+1)\rho_2-(\gamma-1)\rho_1}\\
&\frac{\rho_1}{\rho_2}=\frac{(\gamma+1)p_1+(\gamma-1)p_2}{(\gamma-1)p_1+(\gamma+1)p_2}\\
&\frac{T_1}{T_2}=\frac{\frac{p_1}{p_2}+\frac{\gamma+1}{\gamma-1}}{\frac{p_2}{p_1}+\frac{\gamma+1}{\gamma-1}}
\end{aligned}\right\} \quad (4)$$

Wave front Mach number is : $Ma_2=\frac{v-v_2}{c_2}$;

Local sonic is: $c_2=\sqrt{\gamma RT}=\sqrt{\gamma p_2/\rho_2}$. Then the shock wave equation can be expressed as follows:

$$\left.\begin{aligned}
&\frac{p_1}{p_2}=\frac{2\gamma}{\gamma+1}Ma_2^2-\frac{\gamma-1}{\gamma+1}\\
&\frac{\rho_1}{\rho_2}=\frac{v_2-v}{v_1-v}=\frac{\frac{\gamma+1}{2}Ma_2^2}{1+\frac{\gamma-1}{2}Ma_2^2}\\
&\frac{T_1}{T_2}=1+\frac{2(\gamma-1)(\gamma Ma_2^2+1)}{(\gamma+1)^2Ma_2^2}(Ma_2^2-1)
\end{aligned}\right\} \quad (5)$$

Wave-after Mach number

$$Ma_1=\left[\frac{(\gamma-1)Ma_2^2+2}{2\gamma Ma_2^2-(\gamma-1)}\right]^{1/2},$$

The above equations also show that the airflow parameter relations before and after the shock wave only decide the wave-front flow Mach number Ma_2 and the specific heat ratio .

Non-ideal properties (such as heat conduction, friction, viscosity) of the medium only affect the thickness of the shock wave, without affecting its strength. It is assumed in the process of gas outburst that spewing gas can maintain the propagation of a shock wave, guaranteeing the continuous flow of the shock wave, therefore the simple shock wave is not attenuated. It is assumed that in the undisturbed roadway area the air is in a stationary state, namely v_2=0 m/s, then $Ma_2=\frac{v}{c_2}$, and we can know that parameters in the undisturbed roadway (roadway pressure p_2, density, specific heat ratio) are constant, $c_2=\sqrt{\gamma RT}=\sqrt{\gamma P_2/\rho_2}$. Expressions of pressure, density ρ_1, and velocity are shown as follows:

$$p_1=p_2+\frac{2\rho_2v^2}{\gamma+1}(1-\frac{c_2^2}{v^2}) \quad (6)$$

$$\rho_1=\frac{\rho_0(\gamma+1)}{\frac{2c_2^2}{v^2}+\gamma-1} \quad (7)$$

$$v_1=\frac{2v}{\gamma+1}(1-\frac{c_2^2}{v^2}) \quad (8)$$

3. MECHANISM ANALYSIS OF GAS ADVERSE CURRENT

When the outburst occurs, the coal gas in the body is released in an instant. Due to the large emission and fast transport, relative movement between high concentrations of gas and fresh air flows occurs. Due to the convection-diffusion function, part of the gas is transferred from the high concentration areas to the fresh air, which makes the concentration of gas in the area of fresh air flow rise, causing gas adverse current, as shown in Figure 3.

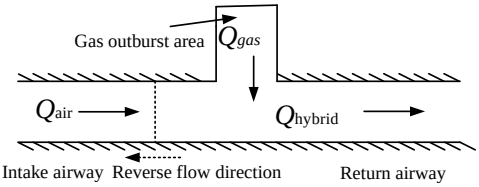

Figure 3: Schematic illustration of gas counter current after outburst.

The theoretical analysis shows that the formation of gas counter current includes two conditions; the volume of gas emission is greater than the air volume after the gas outburst, and the convection diffusion of gas to air. When gas outburst occurs and the volume of gas emission is greater than the volume of the air within the intake airway, the volume within the return airway increases. While in the intake airway, the reverse gas flow pour into the intake airway makes flow volume reduction or flow static, leading to air revering, which is an adverse gas phenomenon. When there is a gas counter-current, there is convection diffusion between fresh air and the high-concentration gas. Convective mass transfer between fresh air and gas occurs, making part of the fresh air gas concentration rise.

After outburst, the gas emission within the intake airway varies. At first, since large coal crushes release a lot of gas instantaneously along with a huge amount of high-pressure gas emission, intake airway

airflow direction is reversed. Gas emission is greatly reduced when outburst ends (Javier T. et.al., 2012). In the absence of sustained energy support, gas flow of the intake airway stops moving or returning to normal air flow. While there is convection diffusion between fresh air and high-concentration gas, gas mass transfers with the air, so the concentration of gas in the fresh air flow rises and re-flux still exists. When the volume of fresh air in the intake airway and the gas emission of outburst areas is stable, the impact scope of the gas to the intake airway is determined, and the concentration of gas within the return airway continues to stabilize. Gas adverse current can be divided into three phases, namely the first stage—entering air retrograde phase, the second stage—diffusion stage, and the third stage—stable dilute phase.

The first stage—entering air retrograde phase: the gas emission is enormous (Wang E.Y. et al., 1996), far greater than the volume of the intake airflow, so flow retrogrades. We can assume that the pressure within the gas flow minus the pressure within the roadway is over-pressure, Δp. In the entering air retrograde phase, we can approximate the retrograde process as the overpressure attenuation process, where the relation is:

$$\Delta p = p_1 - p_2 = \delta W /(sx) \qquad (9)$$

The relation for Δp is as follows:

$$\Delta p = p_1 - p_2 = \frac{\delta}{\varepsilon}\rho_2^{\frac{1}{3}}\left(\frac{W}{s}\right)^{\frac{2}{3}} t^{\frac{3}{2}} \qquad (10)$$

It is important to note that in the place where outburst occurs, the pressure when outburst no longer occurs should be smaller than the pressure at the inlet so as to ensure that under normal circumstances the mine ventilation process, so the pressure difference between the intake airway and the outburst location, is positive. After outburst, the pressure of the outburst shock wave and gas flow that pours into the intake airway is bigger than the pressure of the air which is unaffected by the shock wave and gas flow. The distance of gas retrograde is:

$$x = \delta W / (sp_1' - sp_0) \qquad (11)$$

The second stage—diffusion stage Flores M., 1988: when the counter-current guided by the pressure of gas flow is over, the velocity of the counter-current gas flow is close to zero (Hu W.M. et al., 1998). The phenomenon of gas adverse current is mainly for relative diffusion between gas flow and fresh air. In diffusion, gas flow and air flow can be treated as incompressible fluids. Such gas diffusion meets the conservation of mass and Fick's first law of diffusion .(Jacek S.,2011).

$$J = -D_{AB}\frac{dc_A}{dx} \qquad (12)$$

where D_{AB} is diffusion coefficient (m/s); C_A is volume concentration of gas (/m or kg/m); $\frac{dc_A}{dx}$ is concentration; "–" shows diffusion with the concentration gradient in the opposite direction, namely non-component diffuses from the region of high concentration to areas of low concentration. The unit of J is kg/m s.

$$J_t = J_d + J_i + J_c \qquad (13)$$

where J_t is variation of gas in micro-body per unit time, $J_t = \frac{\partial c_A}{\partial t}dx$; J_d is the net mass flux through gas in the micro-body per unit time, $J_d = -\left[\frac{\partial(uc_A)}{\partial x} + \frac{\partial J}{\partial x}\right]dx$; u is the velocity of air within roadway, u=0m/s; $J_i$is the gas amount of increase or decrease, $J_i = \chi c_A dx$; χ is gas flow attenuation coefficient, $\chi < 1$; J_c is due to a chemical reaction the volume of gas increases or decreases in the micro-body in unit time; while the outburst process of this research does not involve chemical reactions, so $J_c = 0$, then equation (13) can be converted to:

$$\frac{\partial c_A}{\partial t} = -\frac{\partial J}{\partial x} + \chi c_A \qquad (14)$$

The third stage—stable dilute phase: in this phase, the volume of fresh air is much greater than the volume of gas emission. Gas will flow out of the return airway with the flow in a stable manner, and gas concentration tends to be stable after outburst, as shown in Figure 4.

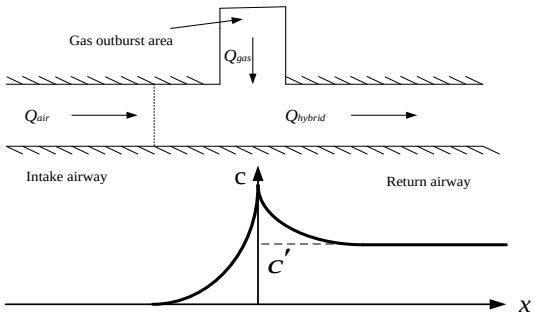

Figure 4: Curves of gas concentration in the laneway at stable dilution stage.

At this time, we focus on the analysis of gas concentration in the return airway, which has certain reference significance to for post-outburst mine rescues. From the above figure, the last stable gas concentration is c' . We can know that:

$$c' = \frac{Q_{\text{gas}}}{Q_{\text{gas}} + Q_{\text{air}}} \qquad (15)$$

4. THE PROPAGATION AND NUMERICAL SIMULATION OF THE OUTBURST SHOCK WAVE AND GAS FLOW WHEN THE OUTBURST PREVENTION DAMPERS FAILS

4.1 Numerical simulation of crossheading and excavation roadway associative

(1)The geometric model

The model is shown as Figure 5. The geometry of the model: a outburst cavity length and breadth are 10 m^3, the excavation roadway is 50 m long, both the total length of intake airway and return airway are 104 m and are relative to the crossheading symmetry. The height of the roadway is 3 m and the width of the roadway is 4 m. Section $B-B'$ is the air inlet side, and section $C-C'$, section $D-D'$ and section $E-E'$ are airflow outlet port. Select a section at a distance crossheading of 25 m as observation points and monitor the change of air pressure, velocity, and gas density.

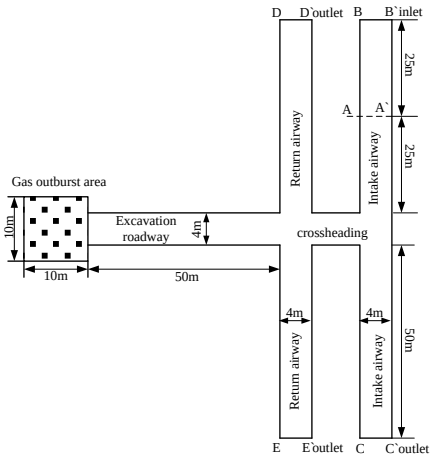

Figure 5: Geometric model numerical simulation of crossheading associated with excavation roadway.

(2) Initial conditions of numerical simulation

In the critical state of outburst, the initial condition of high-pressure gas within outburst region is supposed as:

$$p_1 = 10\text{atm}, u_1 = 0, T_1 = 300\text{K}, C_1 = 1$$

Where P_1 is gas pressure in the outburst region (pressure on the environment set to 1 am), atm; u_1 is velocity, m/s; T is temperature, K; C_1 is relative mass concentration of gas (assumed to be pure methane).

In the critical state of outburst, the initial condition of air within the roadway is supposed as:

$$p_0 = 0\text{atm}, u_0 = 0, T_0 = 300\text{K}, C_0 = 0$$

Where P_0 is gas pressure in the roadway, atm; u_0 is initial velocity within the roadway, m/s. When outburst occurs, due to the great pressure and speed in the roadway, pressure and velocity within the roadway can be approximated as zero; T_0 is temperature within the roadway, K;C_0 is relative mass concentration of gas within the roadway.

The initial condition of the section is supposed as:

$$p_{\text{in}} = 300\text{Pa}, C_{\text{in}} = 0$$

Where p_{in} is relative pressure of cross-section $B-B'$; C_{in} is mass concentration of gas in the cross-section $B-B'$.

The initial condition of cross-section $C-C'$, cross-section $D-D'$ and cross-section $E-E'$ is supposed as:

$$p_{out} = 0\ \text{Pa}$$

Where p_{out} is relative pressure of cross-section $C-C'$, cross-section $D-D'$ and cross-section $E-E'$.

(3) Analysis of results of numerical simulation

Figure 6 shows pressure, velocity, and gas concentration variation at the cross-section.

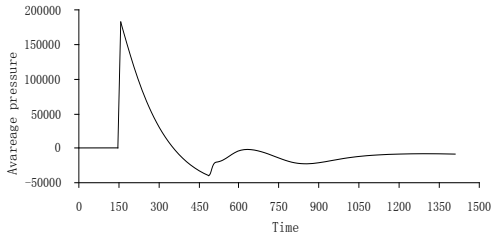

(a) Pressure variation at cross-section A-A`

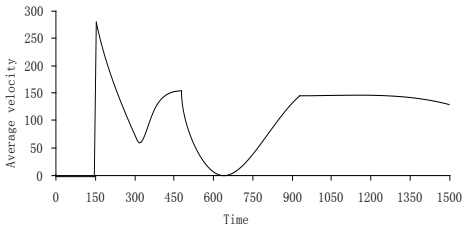

(b) Velocity variation at cross-section A-A`

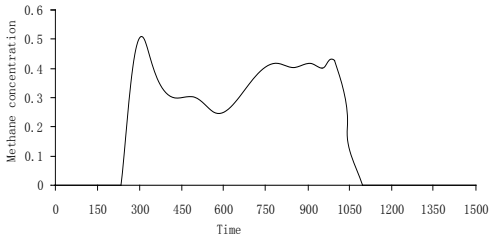

(c) Gas concentration variation at cross-section A-A`

Figure 6: Pressure, velocity, and gas concentration variation at cross-section A-A`.

As shown in Figure 6:

- At 0.156 s, the maximum pressure of the cross-section is 185495.6 Pa, and the maximum speed is 282 m/s.
- At 0.23 s, gas flow reaches the observation point and the cross section of the gas concentration reaches a maximum of 0.499.
- According to the analysis in the 900 cross roadway, gas flow in the concave point begins to return.
- According to the vertical cross-roadway simulations conclusion, assuming that the adsorption of methane in coal and coal powder during shock waves and gas flows movement is no longer flooded, then due to the impact of negative pressure, airflow reflow speed will reach 150 m/s.

Pressure and velocity in the roadway are shown in Figure 7 when gas flow arrives at the observation point section, namely 0.1565 s..

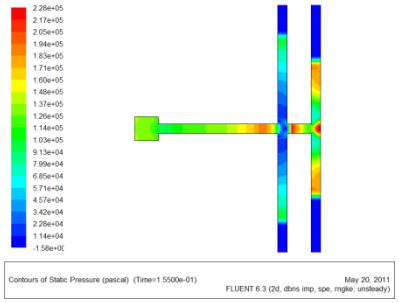

(a) Contour of pressure

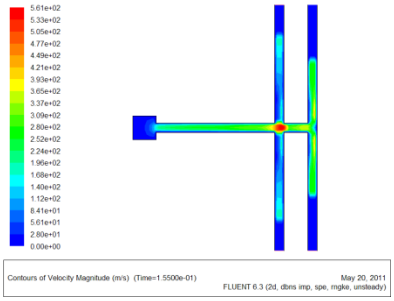

(b) Velocity vector

Figure 7: Contours of pressure and velocity in the roadway at 0.156 s.

As can be seen from Figure 7, the influx of airflow into the intake airway and the pressure and speed of the airflow are greater than the pressure and speed of the return airway. Exporting data can be found from Fluent. The pressure of the return airway is between 0 Pa to 100000 Pa, while the pressure of the intake airway is between 100000 Pa to 200000 Pa. In the return airway flow , the speed of the shock front reaches 200 m/s. In the case of air door damage failure, the impact on the intake airway is greater than on the return airway, but with the throttle prior to the failure, the effects of the shock wave and air flow would obviously be smaller than the return airway in the model of a vertical cross roadway. Because the throttle is damaged, the space of the shock waves and air flows increases and the intake airway and return airway share the influence of shock waves and air flows.

Gas flow reaches the observation point in 0.23 s and leaves in 1.11 s. The concentration of gas within the roadway at 0.23 s, 0.32 s, 0.564 s, and 1.11 s changes as shown in Figure 8.

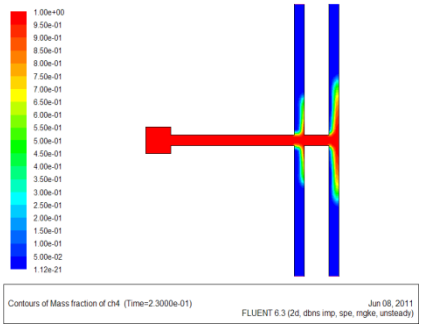

(a) Contour of gas concentration at 0.23 s

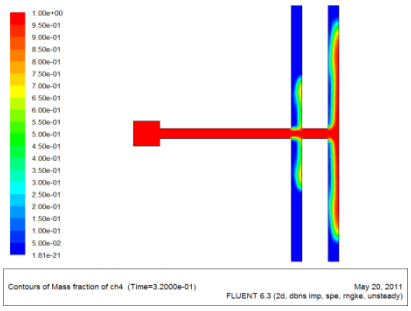

(b) Contour of gas concentration at 0.32 s

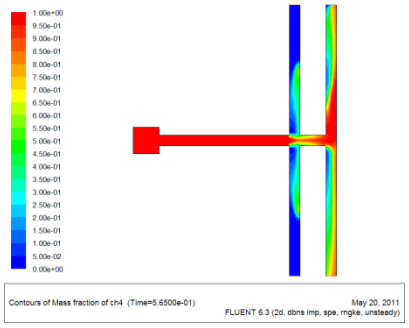

(c) Contour of gas concentration at 0.564 s

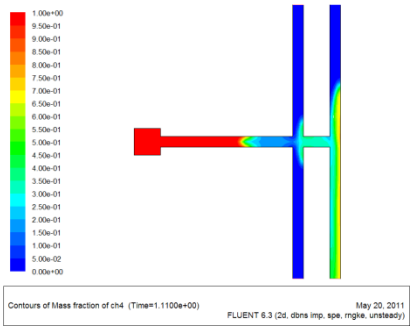

(d) Contour of gas concentration at 1.11 s

Figure 8: Contours of gas concentration in the road way at 0.23 s, 0.32 s, 0.564 s and 1.11 s.

As can be seen from Figure 8, the majority of the gas flows into the intake airway. Only a small part of the gas into the return airway gradually becomes diluted with air and the concentration reduced. Gas flow eventually flows from the high pressure end into the end with the lower pressure, and at this time the concentration in the intake airway is about 0.5. The gas enters the intake airway ultimately along the airflow direction into the mine ventilation system, and the whole mine ventilation systems is subject to the risk of gas explosion.

4.2 Numerical simulation of crossheading and excavation roadway no associative

In order to fix the damage caused by shock wave and gas flow on the intake airway, the most direct approach is to keep the crossheading with the excavation roadway, which may occur not in the same parallel position, and place the air door near the end. It is assumed that the crossheading has an excavation distance of 10 m.

(1)Geometric modelling

The geometric model is shown in Figure 9. The geometric dimensions of the model are described as: the outburst cavity has a side length of 10 m cube; the length of the excavation roadway is 50 m; the length of the intake airway and return airway are 104 m; crossheading is located 10 m above the excavation airway and the distance to section $B-B'$ and section $C-C'$ are 40 m and 60 m respectively; roadway width is 4 m and height is 3 m; section $B-B'$ is flow inlet side, section $C-C'$, section $D-D'$ and section $E-E'$ for flow outlet. Select the section $A-A'$ as the object of observation, monitoring the change of pressure, velocity and gas concentration.

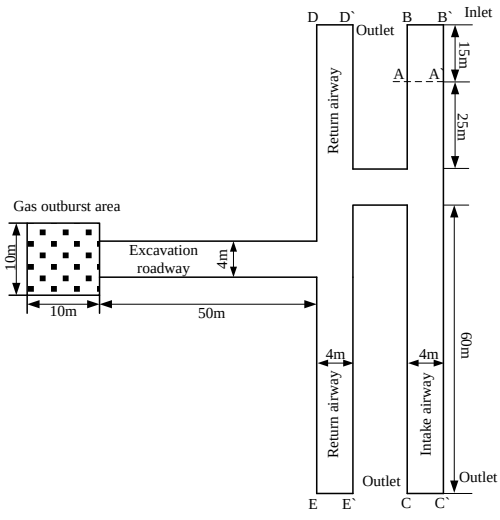

Figure 9: Geometric model numerical simulation of crossheading not associated with excavation roadway.

The initial conditions of the simulation are exactly the same as in the above example. In the critical state of outburst, the initial condition of high-pressure air gas within the outburst cavity is supposed as:

$$p_1 = 10\text{atm}, u_1 = 0, T_1 = 300\text{K}, C_1 = 1$$

Where P_1 is gas pressure in outburst region (pressure on the environment is set to 1 atm), atm; u_1 is velocity, m/s; T_1 is temperature, K; C_1 is relative mass concentration of gas(assuming for pure methane).

In the critical state of outburst, the initial condition of air within the roadway is supposed as:

$$p_0 = 0\text{atm}, u_0 = 0, T_0 = 300\text{K}, C_0 = 0$$

Where P_0 is gas pressure within the roadway, atm; u_0 is initial velocity within the roadway, m/s, when the outburst occurs, due to the great pressure and speed in the roadway, pressure and velocity within the roadway can be approximated as zero; T_0 is temperature within the roadway, K; C_0 is relative mass concentration of gas within the roadway.

The initial condition of section $\text{B}-\text{B}'$ is supposed as:

$$p_{\text{in}} = 300\text{Pa}, C_{\text{in}} = 0$$

Where P_{in} is relative pressure of cross-section $\text{B}-\text{B}'$; C_{in} is mass concentration of gas in the cross-section $\text{B}-\text{B}'$.

The initial condition of cross-section $\text{C}-\text{C}'$, cross-section $\text{D}-\text{D}'$ and cross-section $\text{E}-\text{E}'$ is supposed as:

$$p_{\text{out}} = 0\text{Pa}$$

WhereP_{out} is relative pressure of cross-section $\text{C}-\text{C}'$, cross-section $\text{D}-\text{D}'$ and cross-section $\text{E}-\text{E}'$.

(2)Analysis of results of numerical simulation

Figure 10 shows pressure, velocity and gas concentration variation at cross-section *A-A`*.

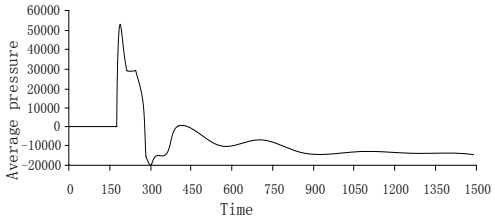

(a) Pressure variation at cross-section A-A`

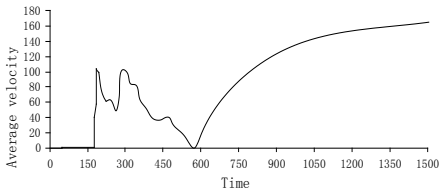

(b) Velocity variation at cross-section A-A`

Figure 10: Pressure and velocity variation at cross-section A-A`.

From Figure 10 and Fluent simulation data we can conclude:

- At 0.19 s, the maximum pressure of the cross-section is 53215.86 Pa, and the maximum speed is 106.7 m/s; compared with the conclusion of the previous section, the gas pressure and speed are greatly reduced, and outburst shock wave and gas flow have less effect on the ventilation system and roadway facilities.
- From the speed change curve in the cross-section it can also be found that when the velocity reverses, namely at 0.57 s, the gas flow direction is reversed.
- After outburst, the counter current speed of theoutburst shock wave and gas flow reaches 160 m/s, which is comparable to the previous section, indicating that crossheading change has little impact on the destruction of counter current air caused by shock wave and gas flow due to negative pressure.

Conditions of the pressure and speed within the roadway are shown as Figure 11:

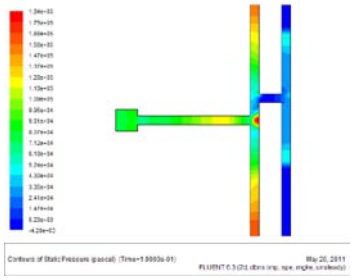

(a) Contours of pressure

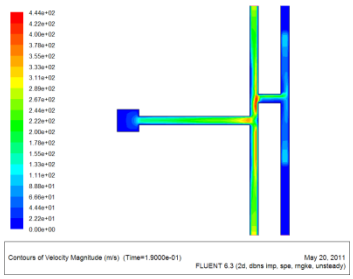

(b) Contours of velocity

Figure 11: Contours of pressure and velocity at 0.19 s.

As can be seen from Figure 11, if crossheading with the excavation roadway is not on the same level, the pressure and velocity of the outburst shock wave and gas flow in the intake airway are far less than in the return airway, and are less affected by the outburst shock wave and gas flow.

Figure 12 shows the concentration variation curves with time at the roadway.

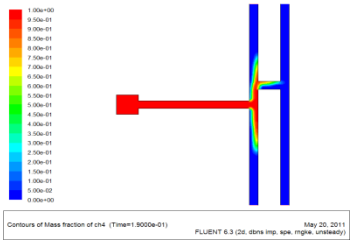

(a) Contours of gas concentration in the roadway at 0.19 s

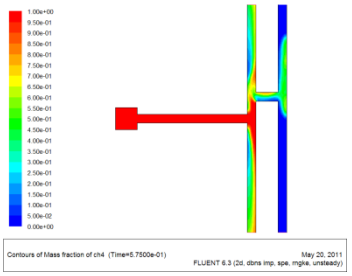

(b) Contours of gas concentration in the roadway at 0.576 s

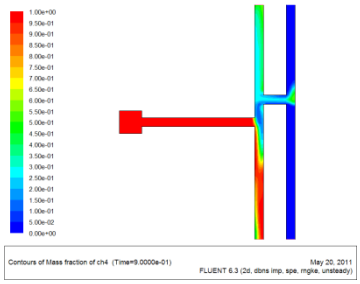

(c) Contours of gas concentration in the roadway at 0.9 s

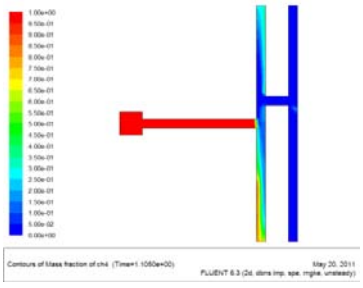

(d) Contours of gas concentration in the roadway at 1.105 s

Figure 12: Contours of gas concentration in the road way at different times.

Figure 12 shows the migration process of gas flow in the outburst. It can be found that most of the emission gas pours out from the cross-section. Due to reflux, gas within the intake airway also pours into the return airway. This shows that if the crossheading is separated from the roadway where outburst occurs and placed near the inlet of the intake airway, then the intake airway is much less affected by the gas flow.

5. CONCLUSIONS

The methane adverse current was divided into three phases: the entering air retrograde phase, the diffusion stage, and the stability of dilute phase. At the different stages, a qualitative analysis of influence scope of the methane adverse current, driving mode, and countercurrent process was performed.

After outburst prevention air door failure, the role of gas flow in mine air flow constantly spreads and can easily induce intake airway gas explosion. When the crossheading and the roadway where outburst occurs are at the same level, most of the gas flow produced by the outburst shock wave and gas flow spreads to the intake airway. When the crossheading and the roadway where outburst occurs at different levels, the gas flow is mainly exhausted from the return airway, and the influence of the intake airway is very small.

6. ACKNOWLEDGEMENTS

The authors are grateful to the State Key Research Development Program of China (2016YFC0801402, 2016YFC0600708), National Natural Science Foundation of China (51474219, 51304213).

7. REFERENCES

Cheng W.Y.,; Liu X.Y and Wang K.J.(2004). Study on regulation about shock-wave-front propagating for coal and gas outburst. Journal of China Coal Society, vol. 29, no. 5, pp. 57-60.

Flores M. (1988). Coalbed methane: from hazard to resource. International Journal of Coal Geology, vol. 35, no. 3, pp. 3-26.

Hu W.M.; Wei J.P and Liu M.J.(1998). Distribution of nonsteady methane in a controlled reciculation system. Journal of China Coal Society, no. 3, pp. 61-66.

Jacek S.(2011). The influence of sorption processes on gas stresses leading to the coal and gas outburst in the laboratory conditions. Fuel, vol. 90, no. 3, pp. 1018-1023.

Javier T. and Susana T.(2012). Eliseo Alvarez. Application of outburst risk indices in the underground coal mines by sublevel caving. International Journal of Rock Mechanics and Mining Sciences, vol. 50, pp. 94-101.

Li S.(2012). Study on dynamic effect of mine ventilation network induced by outburst gas flow[D]. Beijing: China University of Mining & Technology.

María B. and González C.(2007). Control and prevention of gas outbursts in coal mines, Riosa–Olloniego coalfield, Spain. International Journal of Coal Geology, vol. 69, no. 4, pp. 253-266.

Otuonye F. and Sheng J.(1994).A numerical simulation of gas flow during coal/gas outbursts. Geotechnical and Geological Engineering, no. 1, pp. 15-34.

Wang E.Y.; Liang D. and Bo F.S(1996). Study on the mechanism and process of the methane movement it the tunnel. Shanxi mining institute learning journal, vol. 14, no. 2, pp. 24-29.

Wang K.;Li S. and Zhou A.T(2012). Unsteady ventilation network sofaware of mine catastrophic(V1.0): China，2012SR080591[P].

Wang K.; Zhou A.T. and Zhang J.F.(2012). Real-time numerical simulations and experimental research for the propagation characteristics of shock waves and gas flow during coal and gas outburst. Safety Science, vol. 50, pp. 835-841.

Wang K.; Zhou A.T. and Zhang J.F.(2011). Study of the Propagation Characteristics of Shock Wave and Gas Flow during Coal and Gas Outburst at the Roadway with a Right-angled Bend. Journal of China University of Mining & Technology, vol. 40, no. 6, pp. 865-869 .

Wang K.; Zhou A.T. and Zhang P. (2011). Study on the propagation law of shock wave resulting from coal and gas outburst. Journal of Coal Science & Engineering, vol. 17, no. 2, pp. 142-146.

Zhang J. and Sun Y.R.(2007). Study on propagation law of shock wave induced by coal and gas outburst. Mining Safety & Environmental Protection, vol. 34, no. 5, pp. 21-23.

Zhou A.T(2012). Research on propagation characteristics of shock wave and gas flow from gas outburst and induced catastrophic law of mine airflow. Beijing: China University of Mining & Technology.